SUPPLEMENTARY MATERIALS

Joint geodetic and seismic analysis of surface crevassing near a seasonal glacier-dammed lake at Gornergletscher, Switzerland

Louis Garcia[1], Karen Luttrell[1], Debi Kilb[2] and Fabian Walter[3]

1. Dept. of Geology and Geophysics, Louisiana State University, Baton Rouge, LA, USA
2. Scripps Inst. of Oceanography, University of California San Diego, La Jolla, CA, USA
3. Laboratory of Hydraulics, Hydrology and Glaciology VAW, ETH, Zurich

Annals of Glaciology special issue "Progress in Cryoseismology"

The Supplementary Material below includes the following:

- Supplementary Text S1 – S3
- Supplementary Material References
- Supplementary Figures S1 – S8
- Supplementary Tables S1 – S7
- Caption for Supplementary Movie SVideo1, Strain_Video_2006.avi

SUPPLEMENTARY TEXT

Supplementary Text S1: Processing the continuous 2007 data

An extra pre-processing step is required for the 2007 data because it was recorded continuously (*i.e.,* not in trigger mode as in the other years). The storage algorithm for these 2007 data saves 10-second data-packets with 1-2 second overlaps. After collection an auto processing script is applied to each 10-second data-packet to identify icequakes using a short-term-average to long-term-average (STA/LTA) algorithm using 80 units for the short-term average and 800 units for the long-term average (Walter et al., 2009). It is possible that the auto-detection program can identify an icequake twice if the icequake occurred in the duplicated time period. To identify duplicate entries, we scan the detection catalog for consecutive icequakes occurring within 2-seconds of each other. For each consecutive pair identified we cross correlate their waveforms at one representative station. If the correlation is 1.0, indicating a perfect match, these waveforms are flagged as a duplicate pair. Of the two waveforms we select the waveform most centered within the 2-second data-packet and tag the other waveform for removal. Using this process, we eliminated 10,965 duplicate waveforms and maintained a total of 91,800 waveforms (*i.e.,* ~12% were duplicates).

Supplementary Text S2: Gornersee drainage mechanisms

The triggering and drainage mechanisms of Gornersee vary from year to year (Roux et al., 2010). In general, drainage of the Gornersee can be categorized as:

(1) Subglacial: The onset of the drainage is very rapid as the water is routed through the basal hydraulic network, which connects to the lake below its water surface. This type of drainage is often initiated by the complete or partial floatation of damming ice, which provides a sudden connection to the subglacial drainage system. After this connection is established, ice-walled conduits quickly increase their cross-section due to friction melt (Nye, 1976; Spring and Hutter, 1981; Ng and Björnsson, 2003; Clarke, 2003).

(2) Supraglacial: This type of drainage occurs when a glacier overspills the damming ice. The draining water then flows out over the surface of the ice until it enters a moulin (a hydraulic connection between the glacier surface and the subglacial drainage system). This supraglacial water flow incises a channel into the ice surface at a lower rate than the subglacial or englacial channel enlargement (Werder and others, 2010). Lake discharge is consequently slower.

(3) Englacial: This drainage mode is similar to the subglacial drainage, except that lake outflow beneath the water surface connects to the subglacial drainage channel only after flowing through a substantial section of englacial drainage channels at intermediate depths between the surface and the glacier bed.

The details of Gornersee drainage during study years 2004, 2006, and 2007 are described in Table S1.

Supplementary Text S3: Strain rate observations in the early to mid season

We find the early season strain rates in 2006 in our study area increase from a mean of ~200 to ~400 x 10^{-6} d^{-1} (0.07 to 0.14 strain/yr) with strong diurnal variations of 200 – 500 x 10^{-6} d^{-1} (Figure S2). For all three triangles, the principal extension axis is oriented at ~100ºEofN with diurnal variations of ~10º in the northern and southern triangles and diurnal variations of ~20º in the central triangle. In 2007 (Figure S3), the strains in the eastern and western triangles vary around 400 x 10^{-6} d^{-1}, maintaining a strong diurnal signal although regular data gaps during this time make these data more difficult to interpret. Strains in the central triangle are consistently lower, ~200 x 10^{-6} d^{-1}. The principal extension axis in the eastern triangle closest to the lake is oriented ~ 90ºEofN, while the extension axis of the central triangle is oriented ~120ºEofN with much larger diurnal variations of ~45º. The far western triangle down glacier has principal extension at ~45ºEofN with diurnal variations of ~20º. Overall this early to mid-season behavior is consistent with the general observations made from icequakes and GPS displacement, though it clearly demonstrates that the crevasses experience significant diurnal variations in strain along with broad spatial variations in strain.

SUPPLEMENTARY MATERIAL REFERENCES

Clarke, G.K.C., 2003, Hydraulics of subglacial outburst floods: new insights from the Spring- Hutter formulation: Journal of Glaciology, v. 49, p. 299–313.

Ng, F., and Björnsson, H., 2003, On the Clague-Mathews relation for jökulhlaups: Journal of Glaciology, v. 49, p. 161–172, doi: 10.3189/172756503781830836.

Nye, J.F., 1976, Water Flow in Glaciers: Jökulhlaups, Tunnels and Veins: Journal of Glaciology, v. 17, p. 181–207, doi: 10.1017/S002214300001354X.

Roux, P.F., Walter, F., Riesen, P., Sugiyama, S., and Funk, M., 2010, Observation of surface seismic activity changes of an Alpine glacier during a glacier-dammed lake outburst: Journal of Geophysical Research: Earth Surface, v. 115, doi: 10.1029/2009JF001535.

Spring, U., and Hutter, K., 1981, Numerical studies of jökulhlaups: Cold Regions Science and Technology, v. 4.3, p. 227–244.

Walter, F., Dreger, D.S., Clinton, J.F., Deichmann, N., and Funk, M., 2009, Evidence for near-horizontal tensile faulting at the base of Gornergletscher, Switzerland: Mitteilungen der Versuchsanstalt fur Wasserbau, Hydrologie und Glaziologie an der Eidgenossischen Technischen Hochschule Zurich, v. 100, p. 35–60, doi: 10.1785/0120090083.

Werder, M.A., Schuler, T. V., and Funk, M., 2010, Short term variations of tracer transit speed on alpine glaciers: Cryosphere, v. 4, p. 381–396, doi: 10.5194/tc-4-381-2010.

SUPPLEMENTARY FIGURES

Fig. S1. Waveform cross-correlation examples. Each waveform is 0.5 seconds long and the cross-correlation value of the waveform pair is listed (xcorr value). (a) Waveform cross-correlation pairs exhibiting high correlations (>95% as required in this study). (b) Waveform cross-correlation pairs with cross-correlations below 95% (not acceptable for this study).

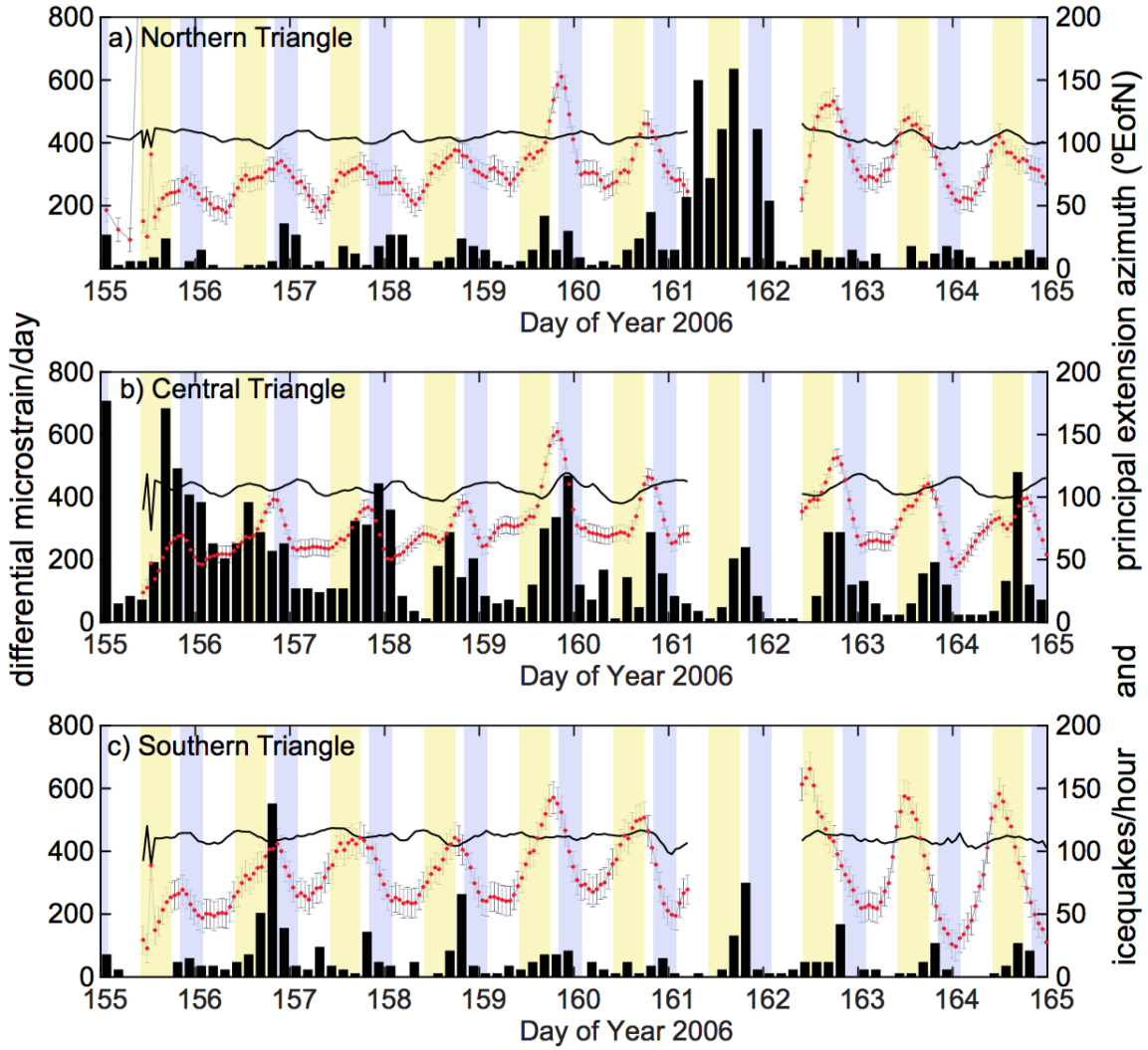

Fig. S2. Data from 2006. Differential strain rate (red line with error bars), azimuth of principal extension axis in degrees East of North (black line), and icequake productivity (histogram) for (a) northern, (b) central, and (c) southern strain triangles, as indicated in Figure 1e. Yellow and blue shaded regions indicate daytime and nighttime periods, as defined in text. Note that diurnal strain peaks during the daytime in all triangles.

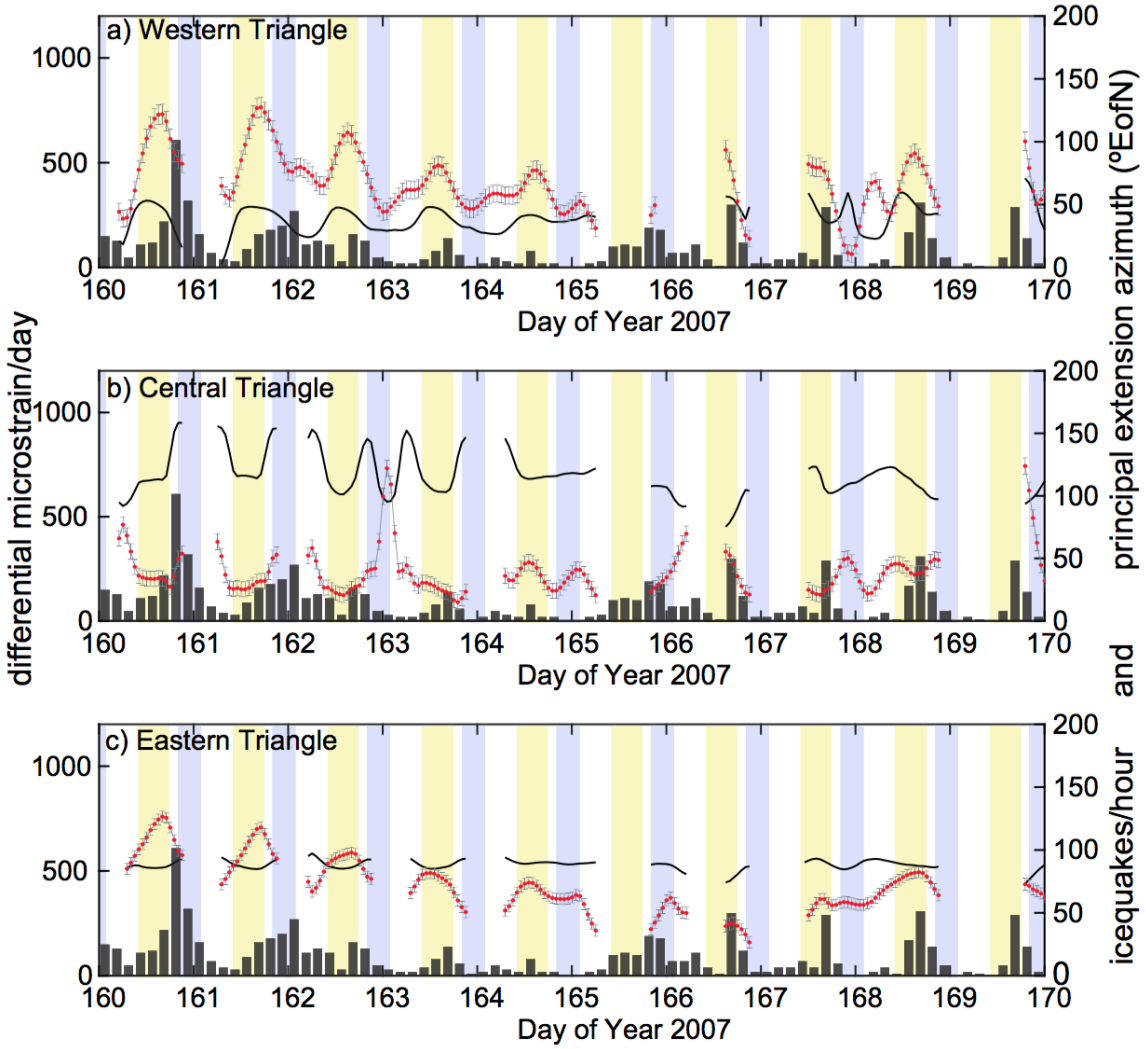

Fig. S3. Data from 2007. Differential strain rate (red line with error bars), azimuth of principal extension axis in degrees East of North (black line), and icequake productivity within each triangle (histogram) for (a) western, (b) central, and (c) eastern strain triangles, as indicated in Figure 1f. Yellow and blue shaded regions indicate defined daytime and nighttime periods, as defined in text. Note that diurnal strain peaks during daytime in eastern triangle and during nighttime in central triangle. Note that because the geodetic and seismic networks in this year were adjacent and did not overlap, histograms of icequake productivity in these plots are calculated from the entire region to compare general productivity as a function of time, rather than limited to an individual strain triangle.

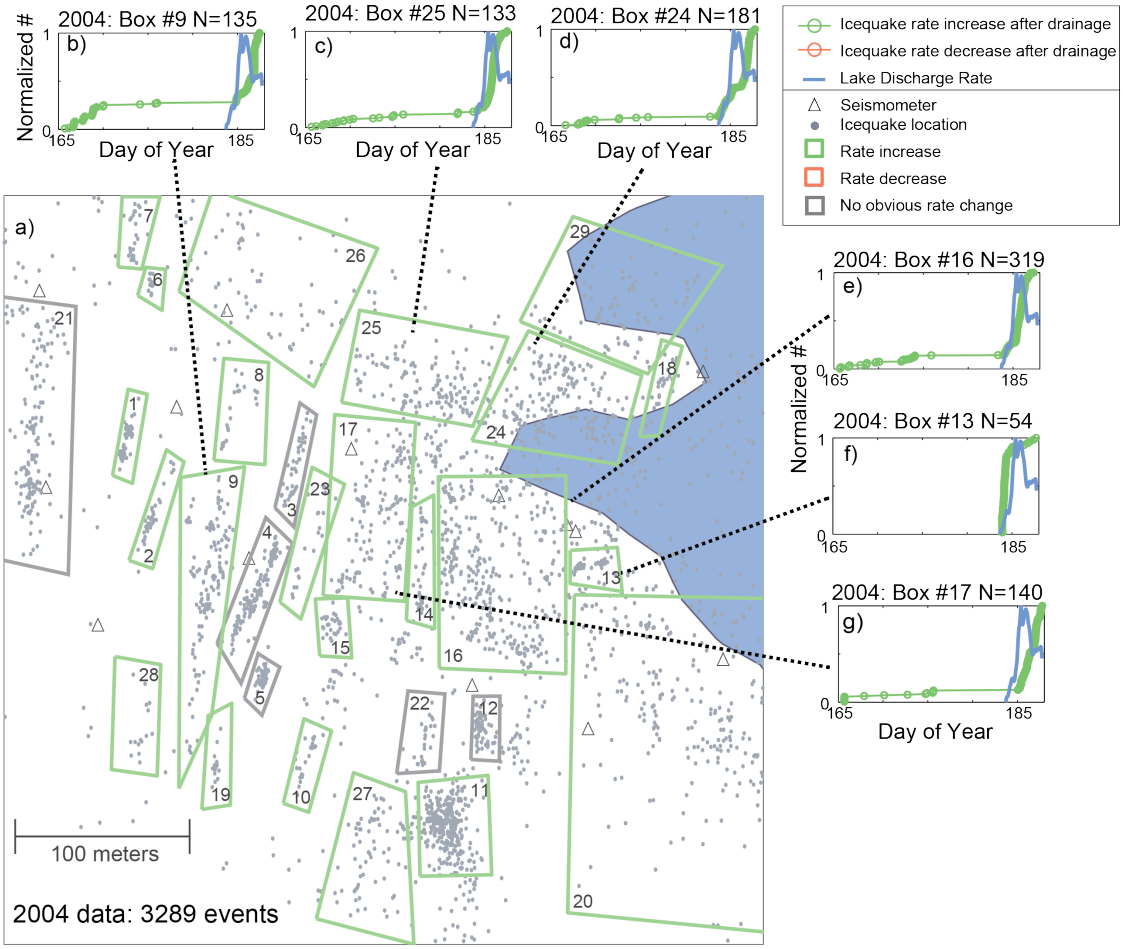

Fig. S4. Data from 2004. (a) Map of 3289 icequakes (grey dots) and seismic station locations (triangles). Boxes outline 29 sub-regions. (b – g) normalized lake discharge rates (blue) and normalized icequake rates (green) within select sub-regions. Subplot headings indicate the year of recording, the box identification number (listed on map) and the total number of icequakes listed as "N=". Here, we show only a small sample of results depicting clear increases in seismicity rates (green cumulative number of icequake vs. time and green boxes on map). The 2004 data show only seismicity rate increases (i.e., no clear decreases).

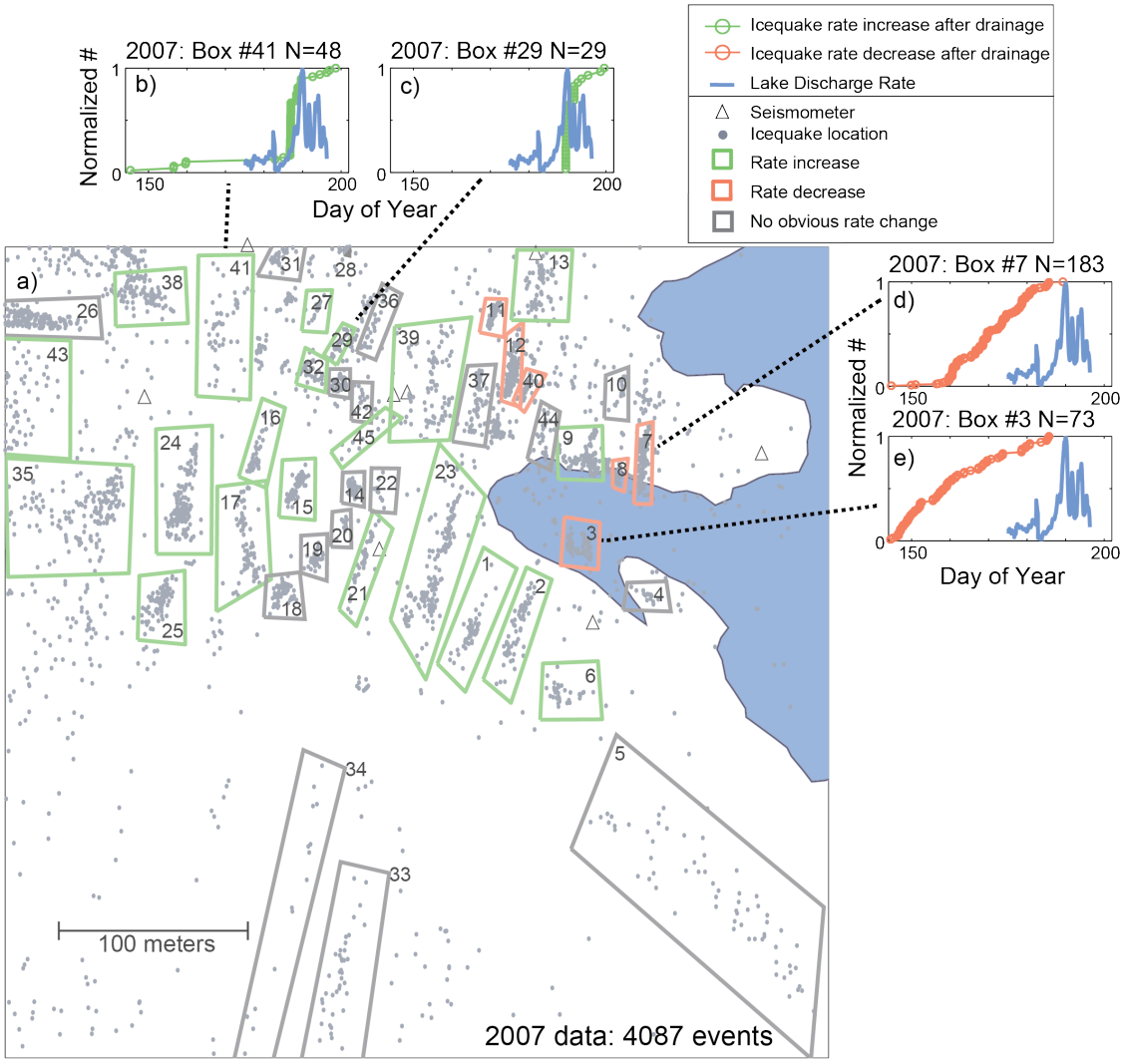

Fig. S5. Data from 2007. (a) Map of 4087 icequakes (grey dots) and seismic station locations (triangles). Boxes outline 45 sub-regions. (b – e) normalized lake discharge rates (blue) and normalized icequake rates (green (red) indicate icequake rate increase (decrease) following drainage) within select sub-regions. Subplot headings as in Figure S4. Here, we show only a small sample of results depicting clear increases in seismicity rates (green cumulative number of icequake vs. time and green boxes on map) and clear decreases in seismicity rates (red cumulative number of icequake vs. time and red boxes on map).

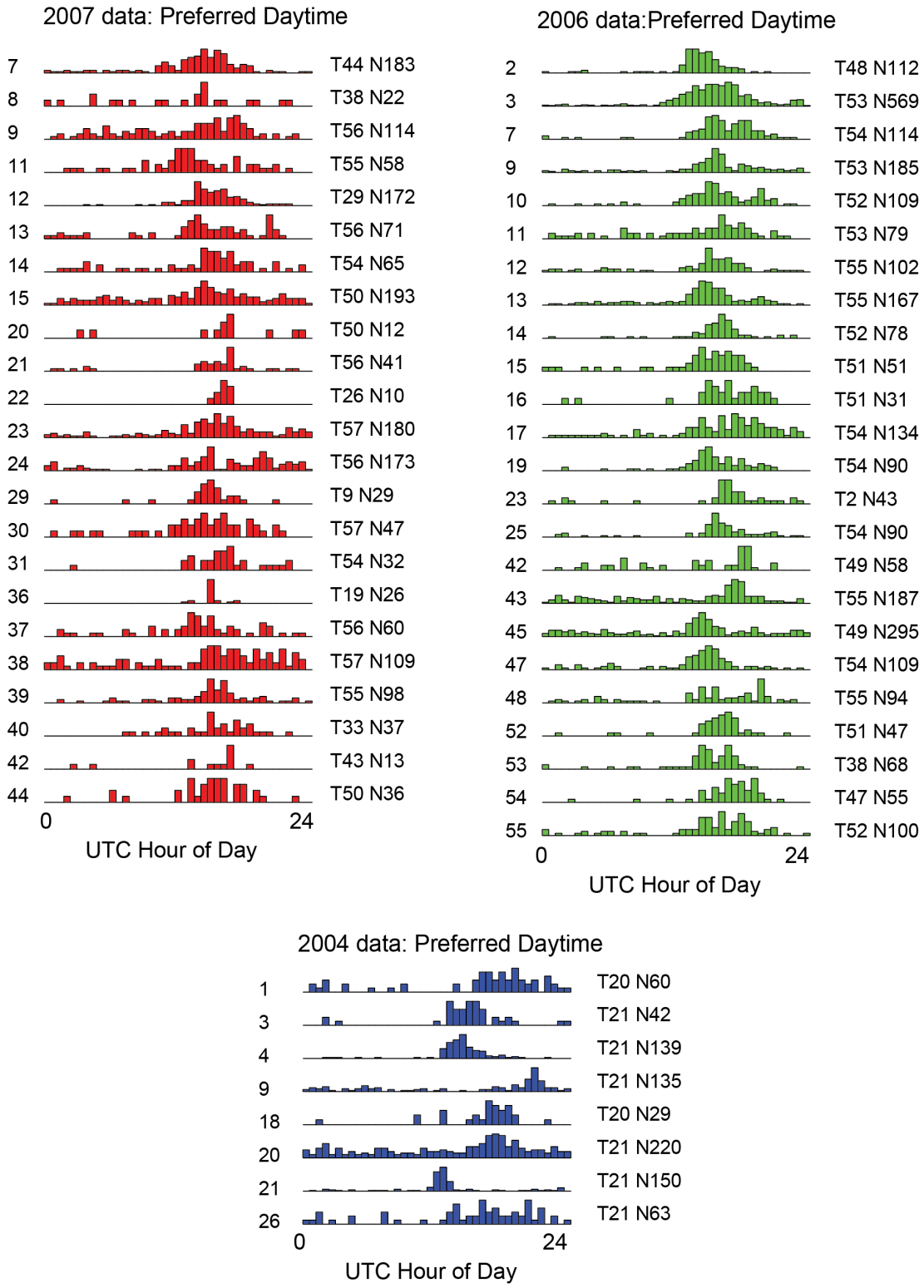

Fig. S6. Histograms of time-of-day of rupture for individual data subsets (box number listed at left; time span of data in days and number of events listed on right) for boxes that show a strong prevalence of icequake occurrence during the daytime. See Figures S2, 5 and S3 for box locations and box numbers for the 2004, 2006 and 2007 data, respectively. Data from 2007 (red), 2006 (green) and 2004 (blue).

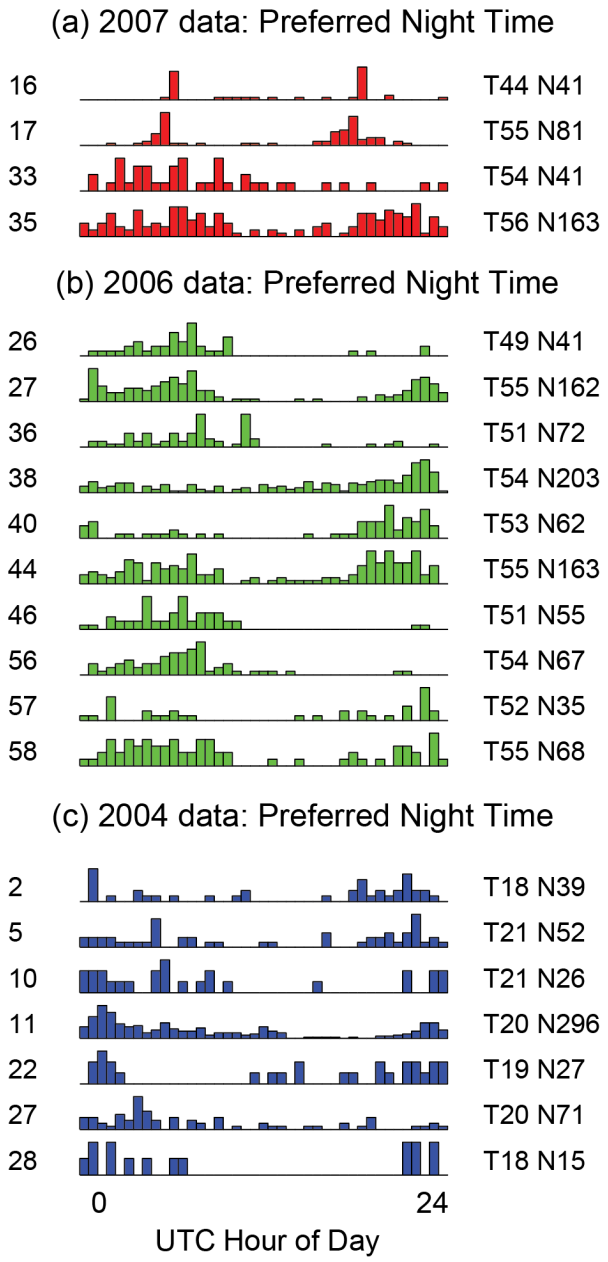

Fig. S7. As in Figure S6 for data that show a preference for icequake occurrence during the nighttime. See Figures S2, 5, and S3 for box locations and box numbers for the 2004, 2006 and 2007 data, respectively.

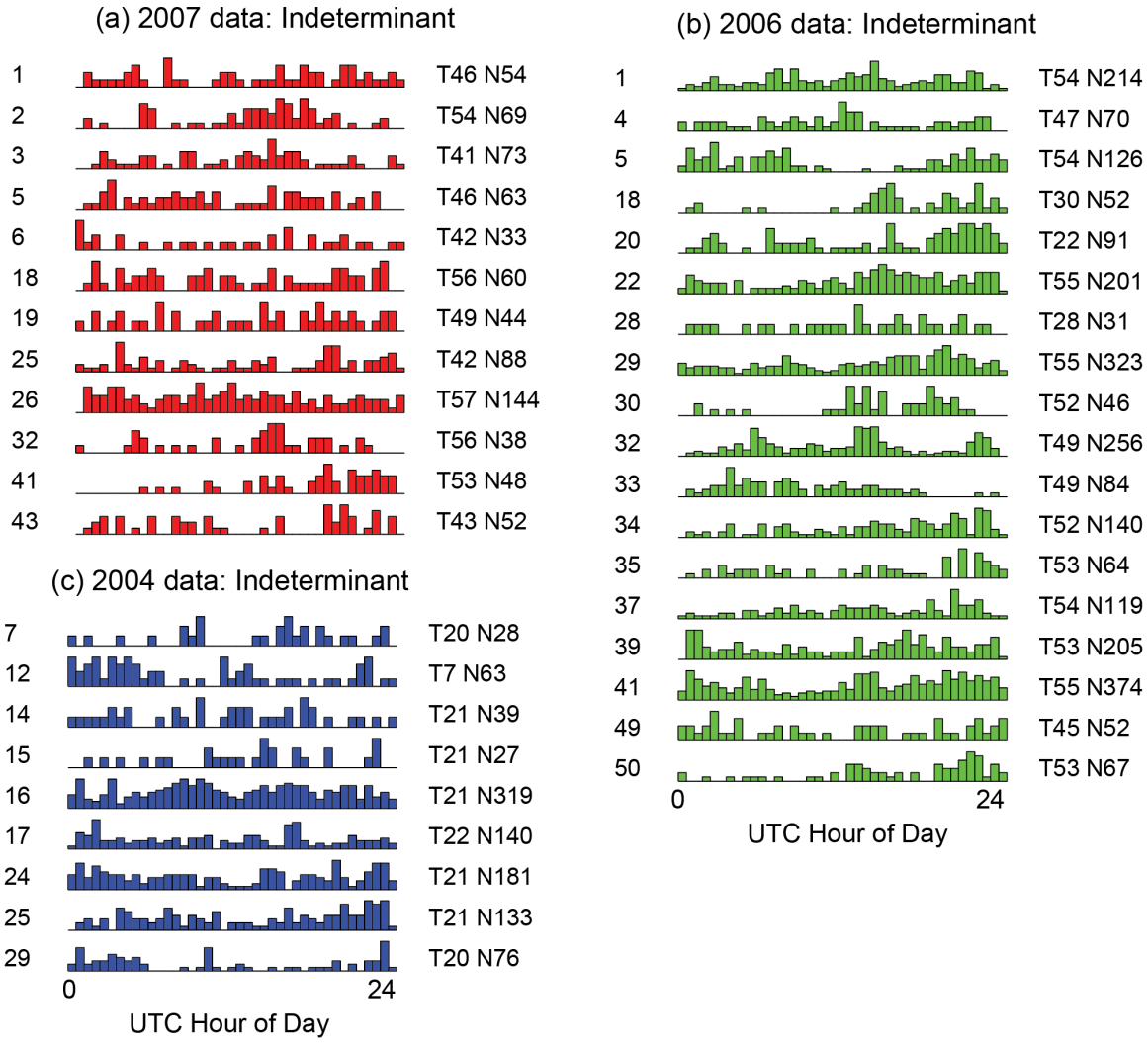

Fig. S8. As in Figures S6-S7 for data that show no preference for either daytime or nighttime icequake occurrence. See Figures S2, 5, and S3 for box locations and box numbers for the 2004, 2006 and 2007 data, respectively.

SUPPLEMENTARY TABLES

Table S1. Positions and types of seismic receivers used in this study

Year	Station ID	Make	Latitude	Longitude	Elevation (m)
2004	G4A1	Lennartz LE-3D	45.9695697	7.80491306	2537.6
2004	G4A2	Lennartz_LE-3D	45.9680859	7.80505149	2538.3
2004	G4A3	Lennartz_LE-3D	45.9677320	7.80405065	2545.3
2004	G4A4	Lennartz_LE-3D	45.9679588	7.80319558	2547.3
2004	G4A5	Lennartz_LE-3D	45.9689359	7.80339818	2539.2
2004	G4A6	Lennartz_LE-3D	45.9687497	7.80396585	2540.2
2004	G4A7	Geospace_GS-20D	45.9687850	7.80390029	2439.3
2004	G4B1	Lennartz_LE-3D	45.9698977	7.80139595	2541.7
2004	G4B2	Lennartz_LE-3D	45.9700029	7.80000982	2542.4
2004	G4B3	Lennartz_LE-3D	45.9689890	7.80005086	2547.9
2004	G4B4	Lennartz_LE-3D	45.9682780	7.80043059	2550.9
2004	G4B5	Lennartz_LE-3D	45.9686181	7.80155001	2547.3
2004	G4B6	Lennartz_LE-3D	45.9691796	7.80230971	2539.1
2004	G4B7	Lennartz_LE-3D	45.9694006	7.80101983	2543.7
2006	G6F1	Geospace_GS-11D	45.9693426	7.80529727	2525.2
2006	G6F2	Geospace_LE-3D	45.9683278	7.80535111	2530.4
2006	G6F3	Geospace_GS-11D	45.9677444	7.80440032	2534.9
2006	G6F4	Lennartz_LE-3D	45.9683206	7.80423905	2535.6
2006	G6F5	Lennartz_LE-3D	45.9690925	7.80365336	2531.2
2006	G6F6	Lennartz_LE-3D	45.9687875	7.80423443	2533.7
2006	G6F7	Lennartz_GS-20D	45.9687282	7.80421339	2492.2
2006	G6F8	Lennartz_LE-3D	45.9699233	7.80405237	2532.9
2006	G6G1	Geospace_LE-3D	45.9702222	7.80174126	2546.0
2006	G6G2	Geospace_LE-3D	45.9699256	7.80028667	2536.7
2006	G6G3	Geospace_GS-11D	45.9692311	7.80030788	2538.0
2006	G6G4	Lennartz_LE-3D	45.9691875	7.80125837	2539.3
2006	G6G5	Lennartz_GS-11D	45.9685315	7.80244215	2534.5
2006	G6G6	Lennartz_LE-3D	45.9692219	7.80257961	2533.6
2006	G6G7	Lennartz_GS-20D	45.9696166	7.80152309	2389.1
2006	G6G8	Lennartz_LE-3D	45.9695863	7.80146355	2533.7
2006	G6H1	Geospace_GS-11D	45.9685035	7.80107968	2540.9
2006	G6H2	Geospace_LE-3D	45.9680457	7.79994659	2549.5
2006	G6H3	Geospace_LE-3D	45.9670686	7.79972858	2550.8
2006	G6H4	Lennartz_LE-3D	45.9670056	7.80085563	2553.8
2006	G6H5	Lennartz_GS-11D	45.9666346	7.80210575	2548.2
2006	G6H6	Lennartz_LE-3D	45.9678604	7.80247123	2544.7
2006	G6H7	Lennartz_GS-20D	45.9674941	7.80086015	2301.2
2006	G6H8	Lennartz_LE-3D	45.9674348	7.80081847	2552.1
2007	G7J1	Geospace_GS-11D	45.9694960	7.80490096	2527.9
2007	G7J2	Geospace_GS-11D	45.9686937	7.80374487	2527.4
2007	G7J3	Geospace_GS-20D	45.9690484	7.80229206	2529.5
2007	G7J4	Lennartz_GS-11D	45.9697785	7.80069594	2528.8
2007	G7J5	Lennartz_LE-11D	45.9704995	7.80140251	2539.7
2007	G7J6	Lennartz_LE-11D	45.9704554	7.80336831	2543.9
2007	G7J7	Lennartz_GS-20D	45.9697829	7.80239499	2412.5
2007	G7J8	Lennartz_GS-11D	45.9697943	7.80248666	2533.3

Table S2. Seismic data recording and waveform selection parameters for each year

Year	Recording Days	Number of stations	Sampling Frequency	Recording Method	Waveform length (seconds)	Number of events	% events used (of total events)
2004	Jun 14 – Jul 08 (25 days)	13	1000 Hz	Trigger	2	2924	8% (~35,000)
2006	May 28 – Jul 23 (57 days)	21	4000 Hz	Trigger	1	7822	15% (~52,000)
2007	May 25 – Jul 22 (59 days)	7	1000 Hz	Continuous	2	3782	4% (~91,000)

Table S3. Initial locations of the GPS stations used in this study

Year	Station ID	Latitude	Longitude	Elevation (m)
2004	14	45.9721376	7.7811219	2506.8
2004	24	45.9700225	7.7908886	2531.7
2004	42	45.9706812	7.8035365	2558.8
2006	14[a]	45.9720171	7.7808776	2497.9
2006	24	45.9693095	7.7925879	2532.8
2006	34	45.9691543	7.8011757	2539.3
2006	45	45.9673258	7.8056270	2535.9
2006	63	45.9728521	7.7715254	2455.0
2006	72	45.9696319	7.8049141	2531.8
2006	73	45.9682909	7.8054977	2527.6
2006	75	45.9669252	7.8003980	2552.3
2007	24	45.9693163	7.7926549	2526.7
2007	34	45.9689231	7.8006229	2537.7
2007	36	45.9663157	7.8022911	2550.4
2007	37	45.9663945	7.7981483	2546.0
2007	44	45.9688534	7.8040727	2527.2

[a] Station 14 in 2006 is omitted from this analysis due to poor data quality

Table S4. Geodetic data recording parameters for each year

Year	Recording Days	Number of stations	Sampling Rate[a]	2006 GPS Sampling Rates[b]		
				Stations 45, 73, 72	Stations 24, 34, 63, 75 (days 155-185)	Stations 24, 34, 63, 75 (days 186-200)
2004	Apr 3 - Sep 12 (161 days)	3	3 hours	--	--	--
2006	May 29 - Jul 26 (57 days)	7	--	3 hours	3 seconds	3 hours
2007	May 26 - Jul 26 (61 days)	5	2 minutes	--	--	--

[a] In 2004 and 2007, sampling was constant for all stations throughout the season
[b] In 2006, sampling rate varied throughout the season and by station

Table S5. Lake level recording parameters used in this study

Year	Recording Days	Sampling rate
2004	May 24 - Jul 5 (42 days)	10 minutes
2006	May 7 - Aug 17 (102 days)	10 minutes
2007	Apr 14 - Jul 15 (91 days)	1 minutes

Table S6. Temporal partitioning of data into four subsets of the ablation season

Year	Early Season (day of year)	Midseason (day of year)	Drainage (day of year)	Post Drainage (day of year)
2004	163 – 170	175 – 182	183 – 187	188 – 190
2006	155 – 162	179 – 186	187 – 194	194 – 201
2007	155 – 161	178 – 185	186 – 195	195 – 202

Table S7. Changes in glacier speed throughout melt season

Year	Region[a]	Station #	Early Season[b] *Speed (cm/day)*	Before Drainage[b] *Speed (cm/day)*	During Drainage[b] *Speed (cm/day)*	After Drainage[b] *Speed (cm/day)*
2004	Up Glacier	#42	0.9 ± 1.9	0.7 ± 1.6	1.0 ± 1.6	1.9 ± 2.8
2004	Down Glacier	#14	9.9 ± 1.7	7.5 ± 2.7	9.1 ± 3.4	7.5 ± 3.9
2004	Down Glacier	#24	9.2 ± 1.6	8.7 ± 3.1	9.9 ± 4.1	8.2 ± 4.1
2006	Up Glacier	#72	0.7 ± 0.3	0.5 ± 0.1	0.8 ± 0.3	0.4 ± 0.1
2006	Up Glacier	#73	1.2 ± 0.3	1.6 ± 0.1	1.7 ± 0.3	2.1 ± 0.4
2006	Up Glacier	#45	2.5 ± 1.0	2.7 ± 0.3	2.7 ± 0.5	2.3 ± 0.1
2006	Down Glacier	#34	5.0 ± 1.7	4.4 ± 0.8	4.8 ± 0.9	5.5 ± 0.4
2006	Down Glacier	#75	8.0 ± 2.7	6.7 ± 1.3	11 ± 1.8	8.6 ± 0.2
2006	Down Glacier	#24	4.0 ± 2.1	4.6 ± 1.3	5.6 ± 3.2	4.9 ± 0.2
2006	Down Glacier	#63	8.8 ± 3.2	4.8 ± 0.9	7.2 ± 3.8	5.9 ± 0.1
2007	Up Glacier	#44	1.4 ± 0.7	1.4 ± 0.9	3.3 ± 1.7	2.3 ± 1.0
2007	Down Glacier	#36	9.2 ± 2.1	6.8 ± 1.8	9.6 ± 2.5	7.8 ± 1.6
2007	Down Glacier	#34	7.2 ± 2.0	4.7 ± 1.6	7.4 ± 2.7	5.5 ± 1.5
2007	Down Glacier	#37	9.3 ± 2.2	6.8 ± 1.8	9.6 ± 3.1	6.7 ± 2.2
2007	Down Glacier	#24	6.1 ± 1.9	3.8 ± 1.0	5.5 ± 3.0	3.8 ± 2.0

[a] Up glacier indicates station near lake, down glacier indicates station away from lake

[b] For precise date range, see Table S6

SUPPLEMENTARY MOVIE

SVideo1. Temporal and spatial evolution of the 2006 data

Movie of the temporal and spatial evolution of the 2006 icequake data and 2006 GPS stations. The Gornersee lake (blue) and GPS stations (small triangles) and the triangular configuration of the GPS stations used to compute strains (large triangles). Boxed text to the east of the lake indicates if the data is from the day or the night, and when the lake is draining. Strain axes are shown as red (principal extension) and blue (principal compression), and red arrows indicate direction and relative magnitude of the GPS station velocity at that location. The temporal evolution of the icequakes are shown in 1-day moving windows. The current one-hour of icequake data are initially depicted as red stars, which fade to white over the next 24-hour period. A date-stamp is used as the title of each movie frame.